International Journal of Cancer

A bi-paratopic anti-EGFR nanobody efficiently inhibits solid tumour growth

For Peer Review

Journal:	*International Journal of Cancer*
Manuscript ID:	IJC-10-2796.R1
Wiley - Manuscript type:	Cancer Therapy
Date Submitted by the Author:	22-Feb-2011
Complete List of Authors:	Roovers, Rob; Utrecht University, Faculty of Science, Department of Biology, Cellular Dynamics Vosjan, Maria; Vumc Laeremans, Toon; Ablynx NV el Khoulati, Rachid; Utrecht University, Faculty of Science, Department of Biology, Cellular Dynamics de Bruin, Renée; Utrecht University, Faculty of Science, Department of Biology, Cellular Dynamics Ferguson, Kathryn; University of Pennsylvania School of Medicine Verkleij, Arie; Utrecht University, Faculty of Science, Department of Biology, Cellular Dynamics van Dongen, Guus; Vumc van Bergen en Henegouwen, Paul; Utrecht University, Faculty of Science, Department of Biology, Cellular Dynamics
Key Words:	EGFR, nanobody, tumour, targeted therapy, signalling

SCHOLARONE™
Manuscripts

A bi-paratopic anti-EGFR nanobody efficiently inhibits solid tumour growth

Rob C. Roovers[1#], Maria J.W.D.Vosjan[2], Toon Laeremans[3], Rachid el Khoulati[1], Renée C.G. de Bruin[1], Kathryn M. Ferguson[4], Arie J. Verkleij[1], Guus A.M.S. van Dongen[2] and Paul M. P. van Bergen en Henegouwen[1]

[1]Utrecht University, Science Faculty, Dept. of Biology, Cellular Dynamics, Padualaan 8, 3584CH Utrecht, the Netherlands

[2]VU University Medical Center, Department of Otolaryngology/Head and Neck Surgery, De Boelelaan 1117, 1081HV Amsterdam, the Netherlands.

[3]Ablynx NV, Technologiepark 21, 9052 Ghent/Zwijnaarde, Belgium

[4]University of Pennsylvania School of Medicine, Department of Physiology, D505 Richards Building, 3700 Hamilton Walk, PA 19104-6085 Philadelphia, U.S.A.

[#]Corresponding author:
phone: +31-30-2539328, Fax: +31-30-2513655, e-mail: r.c.roovers@uu.nl

Running title: A bi-paratopic nanobody for cancer therapy.

Keywords: EGFR, nanobody, tumour, targeted therapy, signalling

For Peer Review

Abstract

The epidermal growth factor receptor (EGFR) has been shown to be a valid cancer target for antibody-based therapy. At present, several anti-EGFR monoclonal antibodies (mAbs) have been successfully used, among which cetuximab and matuzumab. X-ray crystallography data show that these antibodies bind to different epitopes on the ecto-domain of EGFR, providing a rationale for the combined use of these two antibody specificities. We have previously reported on the successful isolation of antagonistic anti-EGFR nanobodies. In the present study, we aimed to improve on these molecules by combining nanobodies with specificities similar to both cetuximab and matuzumab into a single bi-paratopic molecule. Carefully designed phage nanobody selections resulted in two sets of nanobodies that specifically blocked the binding of either matuzumab or of cetuximab to EGFR and that did not compete for each others binding. A combination of nanobodies from both epitope groups into the bi-paratopic nanobody *CONAN-1* was shown to block EGFR activation more efficiently than monovalent or bivalent (monospecific) nanobodies. In addition, this bi-paratopic nanobody potently inhibited EGF-dependent cell proliferation. Importantly, in an *in vivo* model of athymic mice bearing A431 xenografts, *CONAN-1* inhibited tumour outgrowth with an almost similar potency as the whole mAb cetuximab, despite the fact that *CONAN-1* is devoid of an Fc portion that could mediate immune effector functions. Compared to therapy using bivalent, mono-specific nanobodies, *CONAN-1* was clearly more potent in tumour growth inhibition. These results show that the rational design of bi-paratopic nanobody-based anti-cancer therapeutics may yield potent lead molecules for further development.

For Peer Review

Introduction

The epidermal growth factor receptor (EGFR) is a member of a family of four receptor tyrosine kinases (RTK), named Her- or cErbB1, -2, -3 and -4. The EGFR has an extra-cellular domain which is composed of four sub-domains, two of which are involved in ligand binding and one of which is involved in homo- and hetero dimerisation [1, 2], for review, see [3]. EGFR integrates extracellular signals from a variety of ligands to yield diverse intra-cellular responses [4, 5]. The major signal transduction pathway activated by EGFR is composed of the Ras-mitogen-activated protein kinase (MAPK) mitogenic signalling cascade. Activation of this pathway is initiated by the recruitment of Grb2 to tyrosine-phosphorylated EGFR [6, 7]. This leads to activation of Ras through the Grb2-bound Ras-guanine nucleotide exchange factor (GEF) Son Of Sevenless (SOS). In addition, the PI3-kinase-Akt signal transduction pathway is also activated by EGFR, although this activation is much stronger in case there is co-expression of Her3 [8, 9].

The EGFR is implicated in several human epithelial malignancies, notably cancers of the breast, lung, colon, head and neck and brain [10]. Activating mutations in the gene have been found, as well as over-expression of the receptor and of its ligands, giving rise to autocrine activation loops (for review, see [11]). This RTK has therefore been extensively used as target for cancer therapy. Both small molecule inhibitors targeting the receptor tyrosine kinase and monoclonal antibodies directed to the extra-cellular ligand binding domains have been developed and have shown hitherto several clinical successes, albeit mostly for a select group of patients [12].

From the crystal structures of the Fab fragments of several therapeutic monoclonal antibodies in complex with the extra-cellular domain of EGFR [13-15], much knowledge about the working mechanisms of these antibodies has been gathered over the years (for review, see [16]). Most therapeutic antibodies target the ligand binding domain III of the EGFR. One antibody (mAb806) has been reported to recognise an unfolded region of the EGFR that is only exposed when cells either over-express EGFR or express a deletion mutant (de2-7 or vIII) of the receptor [17, 18]. The domain III-specific, therapeutically used antibodies, either occupy EGF contact residues directly (shown for cetuximab and panitumumab [13, 14]), or bind outside the EGF contact area and sterically inhibit the conformational change necessary for receptor activation (as was shown for matuzumab [15]). The effects of the combined use of the

For Peer Review

chimeric mAb cetuximab (derived from murine mAb 225) and humanised mAb matuzumab (derived from the murine mAb 425) on EGFR signalling has recently been investigated and this combination was indeed shown to work well in EGFR inhibition [19].

We have previously reported the generation and use of camelid-derived single domain antibody fragments (termed VHH or Nanobody*) directed to EGFR in therapy of non-established tumours [20]. The single domain nature of these fragments allows for the combination of different nanobodies with different specificities in one molecule: a bi-paratopic nanobody [20, 21] (for review, see [22]). The aim of the current study was to obtain anti-EGFR nanobodies with improved therapeutic efficacy by synthesising bi-paratopic molecules that would combine the specificities of the two domain III specific anti-EGFR antibodies cetuximab and matuzumab. We obtained antagonistic nanobodies that competed for the binding of either cetuximab or matuzumab to the receptor. When combined into one single nanobody format, together with an albumin-binding nanobody for *in vivo* half-life extension [20, 23, 24], this nanobody *CONAN-1* was shown to be a potent receptor antagonist. Importantly, our results show that in a mouse model of established A431 xenografts, this biparatopic nanobody format was very potent in inhibiting tumour outgrowth.

* The term Nanobody® is a registered trademark of Ablynx and is used with permission.

For Peer Review

Materials and Methods

E.coli strain and cell lines

The bacterial strain used was TG1 [25]. The epidermoid squamous carcinoma cell line A431 [26], carrying an amplification of the EGFR gene [27], was purchased from the ATCC (cat. nr. CRL-1555). Her14 cells are derived from NIH 3T3 fibroblasts and stably express roughly 10^5 copies of the human EGFR on their cell surface [28]. The human head and neck squamous cell carcinoma (HNSCC) cell line UM-SCC-14C (14C) was a kind gift of Dr. T.E. Carey, Ann Arbor, MI, USA. All cells were cultured in Dulbecco's Modification of Eagle Medium (DMEM: Gibco, Invitrogen, Paisley, United Kingdom) containing 7.5% (v/v) foetal calf serum and 2 mM L-glutamine in a humidified atmosphere without antibiotics at 37°C under 5% CO_2.

Plasmids and constructs

The cDNA encoding scFv 425 [29], cloned as bispecific single-chain Fv antibody fragment in pSecTag [30] was a kind gift of Dr. Van Beusechem (Department of Medical Oncology, VU University Medical Center, Amsterdam, the Netherlands). The cDNA was re-cloned from pSecTag in a bacterial expression vector identical to pUR5850 [31], except lacking the C-terminal biotinylation sequence (LRSIFEAQKMEW). Induction of protein expression in *E.coli* and purification of scFv from the periplasmic space using IMAC were performed as has been described [25]. The construct encoding the EGFR extra-cellular domain (EGFR-ECD; a.a. 1-614) fused to a human IgG1 Fc gene was a kind gift of Prof. Dr. E.J.J. van Zoelen (Centre for Molecular Life Sciences, Radboud University, Nijmegen, the Netherlands). The construct was used to express EGFR-ECD-Fc fusion protein from an in-house developed expression vector using Hek293E cells. After three days of culture, cellular supernatant was collected and fusion protein was purified by means of prot. G affinity chromatography.

Selection of high affinity- and of cetuximab cross-reactive anti-EGFR nanobodies

EGFR "immune" phage nanobody repertoires used for selections had been synthesised as has been described [20] and were a kind gift of Dr. E.G. Hofman (Cell Biology, Utrecht University, the Netherlands) [32]. Selections were performed on

For Peer Review

recombinant, purified and biotinylated EGFR–ECD (a.a. 1-614, [33]). The protein was biotinylated using biotin amido hexanoic acid 3-sulfo-N-hydroxy succinimide ester (Sigma-Aldrich, Zwijndrecht, the Netherlands). For affinity selections, antigen concentrations used were 100pM, 50pM, 20pM, 10pM and 1pM. Phage (roughly 10^{10} colony forming units (cfu)) and antigen were mixed in a total volume of 100µl PBS containing 1% (w/v) casein and incubated for 3 hours at room temperature (rt) while shaking. For off-rate selection [34], a 100-fold molar excess of non-biotinylated antigen (EGFR-ECD-Fc fusion) was added and incubated for another 3 hours at rt. Phage bound to biotinylated antigen were then captured in an extravidin-coated well (5µg/ml in PBS) of a Maxisorp plate (Nunc, Rochester, U.S.A.) for 15 minutes at rt. Non-bound phage were removed by extensive washing with PBS containing 0.1% (v/v) tween-20 (PBST) and bound phage were eluted with trypsin (1mg/ml in PBS) for 10 minutes at rt. Trypsin was finally inhibited by the addition of ABTS (1mM) and selected phage were used to infect TG1 as described [35].

For the selection of cetuximab-competitive nanobodies, the method of competitive elution [36] was used. Briefly, biotinylated EGFR-ECD (4µg/ml) was captured in a neutravidin-coated (5µg/ml overnight in PBS at 4°C) Maxisorp plate for an hour at rt. Phage were allowed to bind for two hours in (PBS/0.5% (w/v) casein) and plates were subsequently thoroughly washed (as described). Phage bound to overlapping epitopes on EGFR as the one recognised by cetuximab were then eluted by incubation with 200µg/ml cetuximab in PBS for four hours at rt.

Competition ELISA

Maxisorp plates were coated with a rabbit polyclonal anti-human IgG serum (Dako, Glostrup, Sweden; 1:2000 in PBS) over night at 4°C. Next day, wells were washed with PBS, blocked with 2% (w/v) BSA in PBS (PBS/BSA; 30 minutes at rt) and purified EGFR-ECD-Fc was captured at 0.75µg/ml in PBS/BSA for 1 hour at rt. All further incubations were performed in PBS/BSA.

For EGF competition, wells were washed with PBS and a mix of nanobody (either crude periplasmic extract (50% (v/v) in PBS/BSA), or varying concentrations of purified nanobody) in 800pM of biotinylated EGF (Molecular probes/Invitrogen, Carlsbad, U.S.A.) was added. After incubation for 1 hour at rt, wells were washed again and bound EGF was detected with peroxydase-coupled streptavidin (Jackson

John Wiley & Sons, Inc.
For Peer Review

ImmunoResearch Laboratories, Suffolk, England; 1 in 5000 in PBS/BSA) and staining with OPD/H_2O_2.

For cetuximab, mab 425 or nanobody competition, monoclonal phage were prepared as described [35]. Roughly 10^{10} phage were mixed with a 100-fold molar excess of either cetuximab, the 424 scFv or nanobody in 2% (w/v) Marvel (skimmed milk powder) in PBS (MPBS) and the mix was added to coated wells containing the EGFR ECD-Fc in triplicate. Bound phage was detected with a peroxydase-coupled antibody to M13 (Amersham/GE Healthcare, Uppsala, Sweden; 1 in 10000 in MPBS) and staining with OPD/H_2O_2. Optical density was read at 490nm.

Re-cloning and expression of selected Nanobody-genes

The cDNA encoding nanobody Alb1 was made synthetically [37] using the sequence information published in patent WO2006/122786. For the synthesis of bivalent and trivalent nanobodies, nanobody-encoding genes were PCR-amplified using the Expand High Fidelity PCR System (Roche, Mannheim, Germany) with an appropriate primer set, purified, cut with restriction enzymes and cloned into *Sfi*1-*BstE*II cut pUR 5850 [31]. Linker sequences (composed of Gly4-Ser (G_4S) repeats) were encoded in the primers, making it possible to vary the length of the linker separating two nanobody genes. Constructs were sequenced [38] to verify that no mutations were introduced by PCR. Protein expression in *E.coli* TG1 and purification were performed as described [25].

Inhibition of EGFR signalling by selected nanobodies and test for EGFR agonism

The assays measuring the inhibition of EGF-induced EGFR activation by nanobodies and detecting possible agonistic effects of nanobodies on the receptor, were performed as described [20]. As control for the amount of cell lysate loaded, blots were stained for the total amount of either β-actin, or tubulin.

Inhibition of cell proliferation by nanobodies

Measurement of inhibition of cell proliferation by nanobodies or cetuximab using the sulpho-rhodamine B (SRB) assay [39] was performed as described before [20].

Affinity measurements and pharmacokinetics

For Peer Review

Nanobodies were labelled according to the IODO-GEN method [40], as described by Visser *et al.* [41].

For affinity measurements, 14C cells were seeded a day before the assay in 24-well tissue culture plates (Corning, Corning, USA) at 100000 cells per well. ^{125}I-labelled nanobodies were diluted in binding medium (DMEM, containing 7.5% (v/v) FCS, 25mM HEPES and 2% (w/v) Marvel) and added to cells in triplicate. After 2 hours of incubation at 4 degrees, non-bound nanobody was removed by washing twice with ice-cold PBS. Bound nanobody was then quantified by lysis of the cells in 1M NaOH and quantification of the radio-activity using a gamma counter (Wallac, Turku, Finland). Results were analysed with the Graph Pad software.

Measurement of *in vivo* pharmacokinetics with ^{131}I-7D12-9G8-Alb1 was performed in tumour-bearing mice essentially as described [24]. Next to a therapeutic dose of trivalent nanobody (in group 2 in the therapy study, see below), each mouse was injected intra-peritoneally with 0.33 MBq of radio-labelled nanobody (7.5 µg), and blood was drawn at 2 hrs, 6 hrs, 24 hrs, 48 hrs, 72 hrs p.i. to determine detailed pharmacokinetics.

Therapy study

The therapy study was performed essentially as described before [20]. However, therapy was started when tumours were established and the average size of the tumours was approximately 100mm^3. Group1 received PBS twice a week during 5 weeks, group 2 received nanobody and group 3 received cetuximab. Together with the 2nd and 7th dose of nanobody administration, pharmacokinetics were determined in the nanobody-treated group. Anti-tumour effects were expressed by a growth delay factor (GDF), which was defined as the difference in the median time tumours needed to quadruple in the treated group and in the control group, divided by the median quadrupling time of the control group.

For Peer Review

Results

The present study set out to improve the inhibitory capacity of anti-EGFR nanobodies by generating bi-paratopic molecules that are specific for different epitopes on domain III of the EGFR. Therefore, phage nanobody selections were performed using the purified ecto-domain of EGFR as target antigen and 'immune' phage nanobody repertoires [20, 32]. To obtain the different nanobody specificities, we made use of the mAbs cetuximab and matuzumab that were shown to bind to different and non-overlapping epitopes on domain III of the EGFR [13, 15, 16]. We first set out to obtain antagonistic nanobodies with the highest affinity possible, by performing phage selections on very low amounts of biotinylated antigen in solution, combined with "off-rate selections" [34]. When selected nanobody clones were tested for EGF competition, 6 clones (out of 180 clones screened) were found to inhibit the binding of EGF to the EGFR (data not shown). These were subsequently screened for their kinetic dissociation rate constant (k_{off}). Dissociation rate constants were found to vary between 2 and 150 10^{-4} s^{-1} (Table 1A). Because of their low dissociation rate constants, clones 9G8 and 38G7 were then selected for further characterisation (the amino acid sequences of these selected nanobodies can be found in the supplemental data).

After protein production and -purification, the IC50 for EGF binding to EGFR for both nanobodies was measured in ELISA and found to be 6-7 nM for the 9G8 nanobody and 10 nM for the 38G7 nanobody (Fig. 1A). Since the 9G8 nanobody showed a lower IC50 for EGF binding, was expressed to a much higher level in *E.coli* and because the 38G7 amino acid sequence contained some very unusual amino acids at several key positions (data not shown), the 9G8 nanobody was selected for further engineering. To gain insight into the epitope specificity of the selected anti-EGFR antagonists, selected nanobodies were tested for their competition for binding to the EGFR with the whole antibody cetuximab or the scFv of the 425 antibody (matuzumab). Surprisingly, all the selected nanobodies competed with the 425 scFv for binding, but not with cetuximab (shown for 9G8 in Fig. 1B).

We then specifically sought to select nanobodies that would recognise an epitope that overlapped with that of cetuximab by using the method of competitive elution [36] with the antibody cetuximab. Selected nanobodies were subsequently tested for EGF antagonism, as well as for competition with cetuximab for binding to EGFR

For Peer Review

in ELISA. Two nanobodies were selected (called 7C12 and 7D12) that blocked the binding of EGF to the EGFR (Fig. 1A) and indeed competed for the binding of cetuximab and not for that of the scFv of matuzumab (shown for the 7D12 nanobody in Fig. 1C). Based on its lower IC50 for EGF binding (8 *versus* 30nM: Fig. 1A) and lower off-rate (2.5×10^{-3} *versus* 1.5×10^{-2} s^{-1}: Table 1A), the 7D12 nanobody was then selected for further engineering. However, the fact that the 7D12 and 9G8 nanobodies competed for binding to EGFR with two mAbs that do not block each others binding [13, 15], does not necessarily mean that they did not compete for each others binding. To confirm that the 7D12 and 9G8 nanobodies indeed had different epitope specificities, they were tested for competitive binding to immobilised EGFR. Indeed, and as expected, 7D12 and 9G8 did not compete for each others' binding to EGFR (Fig. 1D).

The linking of two nanobody 'heads' into bivalent molecules has already been shown to increase the potency of such molecules [20, 42]. To find the optimal bivalent anti-EGFR nanobody combination, the 7D12 and 9G8 nanobody-encoding genes were re-formatted into bivalent molecules [21] in all possible combinations: either bivalent, mono-specific, or dual-specific / bi-paratopic, using a standard flexible linker of 10 amino acids (in G_4S repeats). The affinities of the monovalent nanobodies, as well as that of the bivalent and bi-paratopic nanobodies were then determined by binding of ^{125}I labelled nanobody to live cells. As expected, bivalent molecules had higher affinities than the corresponding mono-valent counterparts (Table 1B). The mono-specific 7D12-7D12 had the highest affinity, followed by the 7D12-9G8 bi-paratopic molecule.

Subsequently, all constructs were tested for their capacity to inhibit EGF-induced EGFR phosphorylation and EGF-dependent cell proliferation. All nanobodies dose-dependently inhibited the EGF-induced phosphorylation of tyrosine (Y) 1068 of the EGFR (Fig. 2). As phosphorylation of Y1068 of the EGFR has been reported to be the initiation of signalling towards Ras [6], this phosphorylation site of EGFR was measured. The best inhibition was achieved with the bivalent 7D12 nanobody and bi-paratopic molecules 9G8-7D12 and 7D12-9G8. However, the first two showed a slight increase in receptor phosphorylation at the highest nanobody dose used (Fig. 2), a phenomenon that was not observed for the 7D12-9G8 bi-paratopic molecule. These results clearly show that the bi-paratopic anti-EGFR nanobody 7D12-9G8 performed best in inhibiting EGFR signalling.

John Wiley & Sons, Inc.
For Peer Review

When tested for their capacity to inhibit tumour cell proliferation, all nanobodies inhibited the growth of A431 cells (Fig. 3). For comparison, the whole mab cetuximab was used as reference in all experiments. The bi-paratopic nanobody 7D12-9G8 proved as effective as cetuximab in reducing the growth of A431 cells (Fig. 3D). Both bivalent, mono-specific nanobodies 7D12-7D12 and 9G8-9G8 proved less effective in inhibiting the proliferation of A431 cells (Fig. 3A and B) than cetuximab or the 7D12-9G8 nanobody. For both bivalent, mono-specific molecules increased cell proliferation was observed at higher nanobody concentrations, consistent with the observed increased level of EGFR phosphorylation (Fig. 2). Also, mixtures of mono-valent 7D12 and 9G8 or of bivalent 7D12 and bivalent 9G8 were not as potent as the bi-paratopic 7D12-9G8 molecule in inhibiting A431 cell proliferation (Fig. 3). The bi-paratopic 9G8-7D12 molecule also slightly stimulated the growth of A431 cells at low nanobody concentrations, again in agreement with the increased levels of phosphorylated EGFR observed on blot (Fig. 2). These data provide strong support for the choice of the 7D12-9G8 as the most effective, bi-paratopic nanobody combination. In addition, they show that the order of the two 'heads' was critically important for the activity of this bi-paratopic nanobody. Based on these results, the 7D12-9G8 molecule was selected for further optimisation and *in vivo* testing.

An important characteristic of the 7D12-9G8 molecule is the linker length and linker composition connecting the two 'heads'. This linker is supposed to provide sufficient space/length and freedom to allow the two nanobodies to bind ('chelate' [43]) simultaneously to the same EGFR molecule. We therefore analysed the effect of flexible linkers consisting of G_4S repeats varying in length from 5 to 30 a.a.. The resulting bivalent constructs were then tested for their ability to inhibit A431 cell proliferation. Surprisingly, the length of the linker used between the two nanobody "heads" turned out to be almost inversely correlated with the efficacy of the molecule in inhibiting A431 cell proliferation, with 5 and 10a.a. linkers being optimal (Fig. 4A). Therefore, a linker of 10a.a. was chosen as the optimal format for the anti-EGFR 7D12-9G8 bi-paratopic nanobody.

Since the 7D12-9G8 nanobody has a molecular weight of roughly 30 kDa, it would be cleared very rapidly *in vivo* via the kidneys once injected into the blood stream of mice [44]. To prolong the *in vivo* half-life of small proteins, binding to albumin has been reported to be an excellent option [20, 23, 24]. Therefore, the gene

John Wiley & Sons, Inc.
For Peer Review

encoding the anti-MSA/HSA nanobody Alb1 (this nanobody recognises both MSA as well as HSA with a KD of 6.5nM for MSA and 0.57nM for HSA) was made synthetically [37] and fused C-terminally to the bi-paratopic 7D12-9G8 nanobody using two different linker lengths (15 or 30 amino acids in repeats of Gly_4-Ser) between the anti-EGFR nanobodies and Alb1. First, trivalent nanobodies were tested for their functionality in ELISA: the binding of biotinylated MSA to EGFR-bound 7D12-9G8 and 7D12-9G8-Alb1 was assessed and shown to depend on the presence of the Alb1 nanobody (Fig. 4B). These results show that at least one of the anti-EGFR 'heads' together with the Alb1 nanobody present in the same trivalent molecule could simultaneously bind antigen. Since in an *in vivo* (therapy) situation, albumin will be abundantly present, both trivalent nanobodies (containing either a 15- or 30 a.a. linker before the Alb1 nanobody) were then tested for their capacity to inhibit A431 cell proliferation in the presence of 1% (w/v) HSA. The construct containing a 15 amino acid linker before the Alb1 nanobody significantly lost potency in the presence of HSA (data not shown). However, for the construct containing a 30 residue linker between the anti-EGFR units and Alb1 unit, efficacy in inhibition of cell proliferation was not affected by the presence of HSA (Fig 4C). Therefore, this version was selected for further *in vivo* testing and was named COoperative NANobody-1 (*CONAN-1*).

To check whether the *CONAN-1* nanobody by itself did not induce activation of the EGFR, the nanobody was given as ligand at high concentration to EGFR over-expressing cells (Her14 cells). Figure 4D shows that *CONAN-1* did not cause receptor activation in the absence of EGF, while cells readily responded to EGF stimulation. Finally, the *CONAN-1* nanobody was shown to strongly inhibit EGF induced signalling (Fig. 4E): not only was receptor phosphorylation inhibited (Fig. 2), but the phosphorylation of MAPK was also reduced to background levels. These results show that the *CONAN-1* nanobody functioned as a true receptor antagonist and it was therefore tested in an *in vivo* therapy study.

To measure blood pharmacokinetics of the *CONAN-1* molecule, a trace amount of radio-labelled nanobody was injected intravenously (iv) in the tail vein of tumour-bearing mice, together with a therapeutic dose of nanobody. Blood sampling revealed an *in vivo* half-life of approximately 48 hours (Fig. 5A), when fitted to a mono-exponential decay. In a murine model of established A431 human xenografts in athymic mice, the administration of *CONAN-1* intra-peritoneally (ip) as therapy was

For Peer Review

compared with therapy using cetuximab. Based on the measured pharmacokinetics of *CONAN-1* (Fig. 5A), therapy was given twice weekly. *CONAN-1* had an efficacy in inhibiting the growth of established A431 tumours that was largely comparable to that of cetuximab during treatment (Fig. 5B). The mean tumour volume in the cetuximab-treated group diminished slightly after 4 days, up to 2 weeks of treatment (a phenomenon not observed in the nanobody-treated group), but then increased at approximately the same speed as that of the nanobody-treated group. After treatment was stopped, tumours of mice in the nanobody-treated group did not re-grow significantly faster than tumours of mice in the cetuximab-treated group. During therapy, *CONAN-1* induced a significantly stronger effect than cetuximab during the first 6 days, but cetuximab caused a significantly stronger anti-tumour effect after day 8 ($p<0.05$; independent sample T-test). A comparison of the growth-delay factors for quadrupling of the tumour volume revealed that *CONAN-1* induced a strong response in tumour growth inhibition (GDF = 1.52) but that this response was slightly stronger in the group treated with cetuximab (GDF = 2.19: Table 1C). In a separate, equal experimental setup, therapy using the trivalent anti-EGFR nanobody 7D12-7D12-Alb1 was also compared to that using cetuximab. A comparison of the GDF's calculated for both nanobody treatments revealed that *CONAN-1* (GDF = 1.52) induced a much stronger anti-tumour response than the 7D12-7D12-Alb1 nanobody (GDF = 1, Table 1C). Importantly, this proves again that the combination of different paratopes and thereby different modes of EGFR inhibition into a single molecule was superior to the use of mono-specific targeting for EGFR inhibition.

For Peer Review

Discussion

The present study set out to combine nanobodies into a bi-paratopic format in order to improve their efficacy in tumour growth inhibition. The results show the efficacy of the optimised *CONAN-1* nanobody in therapy to be better than that of mono-specific 7D12-7D12-Alb1 and almost equal to that of the well-characterised anti-EGFR mAb cetuximab, although the former is devoid of immune effector functions.

To obtain anti-EGFR nanobodies that recognize non-overlapping epitopes on the ligand binding domain 2 of EGFR (domain III), we made use of two mAbs of which the binding sites were previously shown to be different by crystallography [13, 15]. First, we selected nanobodies for high affinity binding [34]. Surprisingly, these selections only resulted in clones that cross-reacted with the scFv of matuzumab (shown for the 9G8 nanobody in Fig. 1). The nanobodies Ia1, L2-3.40 and IIIa3, previously found using EGF elution [20], were also found to compete for binding to EGFR with the 9G8 nanobody and the 425 scFv (data not shown). The high prevalence of nanobodies recognising the part of domain III also bound by matuzumab is probably a reflection of the immunogenicity of that particular part of the receptor. However, by carefully designed phage nanobody selections, cetuximab cross-reactive nanobodies were readily obtained. These results underline the power of the combination of active immunisation of *Llama*, nanobody repertoire cloning and phage nanobody selections to obtain nanobodies that recognise defined epitopes on a given antigen (for review, see [22]).

Secondly, phage nanobody selections were performed in combination with specific elution using cetuximab. Only two nanobodies were found that blocked binding of EGF to EGFR and that of cetuximab to EGFR: clones 7D12 and 7C12. These nanobodies have previously been described by Gainkam *et al.* [45]. The reported affinity of the 7D12 nanobody (2.3nM: [45]) differs from the affinity value we obtained (10 nM: Table 1B). This discrepancy might well be due to the different methods used to measure the affinity. We deliberately chose for cell binding experiments, as the affinity values obtained by this method are probably more representative for the *in vivo* situation. The EGFR makes numerous contacts with other receptors, integrins and lipids [32] which may shield particular epitopes on the ecto-domain that are accessible in an *in vitro* SPR setup. However, the ^{125}I-labelling of the nanobodies may

For Peer Review

have influenced their affinity, as tyrosines in the antigen binding sites may have been altered, thereby lowering the affinity.

The order in which the two nanobodies were linked together in a bivalent or bi-paratopic molecule was shown to be an important parameter for the efficacy of the anti-EGFR bi-paratopic molecule (Figs. 2 and 3). In addition, the linker composition also strongly influenced the characteristics of the nanobody, as a hinge-derived sequence between 9G8 and 7D12 caused this bi-paratopic molecule to act as a receptor agonist (results not shown). The same phenomenon can slightly be observed for the 9G8-7D12 bi-paratopic nanobody containing a flexible linker and the 7D12-7D12 mono-specific molecule (Fig. 4). The engineering and thorough testing of this type of therapeutic molecules is therefore critically important to avoid artificial receptor activation.

Surprisingly, the 7D12-7D12 bivalent nanobody had the highest affinity, yet was not the most potent in inhibiting tumour cell proliferation (Table 1B and Fig. 3). This may be explained by artificial activation of the EGFR caused by cross-linking of receptors through inter-molecular binding of the nanobody. The 7D12-9G8 nanobody did not cause receptor activation (Figs. 2, 3C and 4D) and therefore functioned as true receptor antagonist. However, simultaneous binding of the two 'heads' in the bi-paratopic nanobody 7D12-9G8 to one and the same EGFR molecule ('chelating' binding [43]) could not be demonstrated. Size exclusion chromatography and cross-linking experiments did not give conclusive results (data not shown). Preliminary X-ray crystallographic data confirm the predicted location of the epitopes of 7D12 and 9G8 (details of co-crystal structures of EGFR fragments with 7D12 and 9G8 will be published separately, Ferguson *et al.*, manuscript in preparation). These structures also suggest that simultaneous binding of both heads of 7D12-9G8 may be possible with a 10 amino acids linker. However, "chelating" binding will be highly dependent on the linker composition. Based on the estimated locations of the C-terminus of 7D12 and N-terminus of 9G8 in these crystal structures, a linker of only 10 amino acids would have to pass very closely to the surface of EGFR. It is conceivable that such a linker does not permit the bi-paratopic nanobody to 'chelate' [43] the EGFR, but that the 7D12-9G8 nanobody binds the receptor with only one 'head' at any given time. However, the presence of the second specificity within the same molecule probably results in fast re-binding once the first nanobody unit dissociates from its epitope, thereby resulting in increased apparent affinity (Table 1B: compare 7D12 and

John Wiley & Sons, Inc.
For Peer Review

9G8 with 7D12-9G8) and increased potency in EGFR inhibition (Fig. 3). Also, binding of the bi-paratopic 7D12-9G8 to EGFR may induce some conformational change and thus an 'induced fit', thereby permitting both 'heads' to bind simultaneously. For the mono-specific, bivalent 7D12-7D12 molecule, simultaneous binding of both 'heads' would require a cluster of receptors, where domain III is available in two adjacent EGFR molecules. Pre-dimers of EGFR in the absence of EGF have been demonstrated [46, 47]. However, the EGFR in such complex will probably not be bound bivalently by 7D12-7D12, since the L2 domains are located on either side of the 'back-to-back' dimer [2], pointing away from each other.

The *in vivo* half-life of the *CONAN-1* nanobody was very comparable to that of a similar nanobody construct described by Tijink *et al.* [24] and to that of directly radio-labelled MSA (data not shown). Since the affinity of the Alb1 nanobody for HSA is even higher than that for MSA (6.5nM (MSA) *versus* 0.57nM (HSA)), it is expected that the *CONAN-1* nanobody would circulate in humans with the same kinetics as that of HSA (its half-life being 10-14 days). The pharmacokinetics would then be very comparable to that of a whole IgG.

Treatment with cetuximab resulted in tumour regression after 4 days, which lasted until approximately day 14 (when tumour started to re-grow). This is indicative of activation of immune effector cells. Despite the fact that the *CONAN-1* nanobody cannot interact with the immune system, its efficacy was largely comparable to that of cetuximab. This could be partially due to better tumour penetration [24] in combination with similar (or even better) pharmacokinetics (Fig. 6 and [24]). The modular nature of nanobodies permits the addition of 'effector' heads (e.g. a nanobody to recruit effector cells); it would be interesting to test such constructs in comparison with cetuximab.

The modularity of nanobodies in combination with the power and possibilities of phage display also permit the synthesis of combinations of nanobodies recognising well-defined epitopes on other receptors (e.g. the combination of nanobodies recognising the pertuzumab- and trastuzumab epitopes on Her2/Neu). Additionally, it permits the synthesis of multi-specific molecules capable of inhibiting two (or even more) signal transduction pathways simultaneously, which may well lead to a higher efficacy of nanobody-mediated therapy. In conclusion, our results show that the rational design and synthesis of multivalent nanobody molecules is a promising option to develop new cancer therapeutics.

For Peer Review

Acknowledgements

We thank the USP/DSP team from the CMC department of Ablynx for production and purification of the CONAN-1 nanobody. We thank Marijke Stigter-van Walsum for excellent technical assistance. R. Roovers and M. Vosjan are supported by STW grant nr. 10074.

For Peer Review

References

1. Garrett TP, McKern NM, Lou M, Elleman TC, Adams TE, Lovrecz GO, Zhu HJ, Walker F, Frenkel MJ, Hoyne PA, Jorissen RN, Nice EC, et al. Crystal structure of a truncated epidermal growth factor receptor extracellular domain bound to transforming growth factor alpha. Cell 2002;110:763-73.

2. Ogiso H, Ishitani R, Nureki O, Fukai S, Yamanaka M, Kim JH, Saito K, Sakamoto A, Inoue M, Shirouzu M, Yokoyama S. Crystal structure of the complex of human epidermal growth factor and receptor extracellular domains. Cell 2002;110:775-87.

3. Ferguson KM. Structure-based view of epidermal growth factor receptor regulation. Annu Rev Biophys 2008;37:353-73.

4. Yarden Y. The EGFR family and its ligands in human cancer. signalling mechanisms and therapeutic opportunities. Eur J Cancer 2001;37 Suppl 4:S3-8.

5. Jorissen RN, Walker F, Pouliot N, Garrett TP, Ward CW, Burgess AW. Epidermal growth factor receptor: mechanisms of activation and signalling. Exp Cell Res 2003;284:31-53.

6. Buday L, Downward J. Epidermal growth factor regulates p21ras through the formation of a complex of receptor, Grb2 adapter protein, and Sos nucleotide exchange factor. Cell 1993;73:611-20.

7. Gale NW, Kaplan S, Lowenstein EJ, Schlessinger J, Bar-Sagi D. Grb2 mediates the EGF-dependent activation of guanine nucleotide exchange on Ras. Nature 1993;363:88-92.

8. Soltoff SP, Carraway KL, 3rd, Prigent SA, Gullick WG, Cantley LC. ErbB3 is involved in activation of phosphatidylinositol 3-kinase by epidermal growth factor. Mol Cell Biol 1994;14:3550-8.

9. Prigent SA, Gullick WJ. Identification of c-erbB-3 binding sites for phosphatidylinositol 3'-kinase and SHC using an EGF receptor/c-erbB-3 chimera. Embo J 1994;13:2831-41.

10. Uberall I, Kolar Z, Trojanec R, Berkovcova J, Hajduch M. The status and role of ErbB receptors in human cancer. Exp Mol Pathol 2008;84:79-89.

11. Robertson SC, Tynan J, Donoghue DJ. RTK mutations and human syndromes: when good receptors turn bad. Trends Genet 2000;16:368.

12. Patel DK. Clinical use of anti-epidermal growth factor receptor monoclonal antibodies in metastatic colorectal cancer. Pharmacotherapy 2008;28:31S-41S.

13. Li S, Schmitz KR, Jeffrey PD, Wiltzius JJ, Kussie P, Ferguson KM. Structural basis for inhibition of the epidermal growth factor receptor by cetuximab. Cancer Cell 2005;7:301-11.

14. Li S, Kussie P, Ferguson KM. Structural basis for EGF receptor inhibition by the therapeutic antibody IMC-11F8. Structure 2008;16:216-27.

15. Schmiedel J, Blaukat A, Li S, Knochel T, Ferguson KM. Matuzumab binding to EGFR prevents the conformational rearrangement required for dimerization. Cancer Cell 2008;13:365-73.

16. Schmitz KR, Ferguson KM. Interaction of antibodies with ErbB receptor extracellular regions. Exp Cell Res 2009;315:659-70.

17. Johns TG, Adams TE, Cochran JR, Hall NE, Hoyne PA, Olsen MJ, Kim YS, Rothacker J, Nice EC, Walker F, Ritter G, Jungbluth AA, et al. Identification of

For Peer Review

the epitope for the epidermal growth factor receptor-specific monoclonal antibody 806 reveals that it preferentially recognizes an untethered form of the receptor. J Biol Chem 2004;279:30375-84.

18. Garrett TP, Burgess AW, Gan HK, Luwor RB, Cartwright G, Walker F, Orchard SG, Clayton AH, Nice EC, Rothacker J, Catimel B, Cavenee WK, et al. Antibodies specifically targeting a locally misfolded region of tumor associated EGFR. Proc Natl Acad Sci U S A 2009;106:5082-7.

19. Kamat V, Donaldson JM, Kari C, Quadros MR, Lelkes PI, Chaiken I, Cocklin S, Williams JC, Papazoglou E, Rodeck U. Enhanced EGFR Inhibition And Distinct Epitope Recognition By EGFR Antagonistic MABS C225 And 425. Cancer Biol Ther 2008;7.

20. Roovers RC, Laeremans T, Huang L, De Taeye S, Verkleij AJ, Revets H, de Haard HJ, van Bergen en Henegouwen PM. Efficient inhibition of EGFR signaling and of tumour growth by antagonistic anti-EFGR Nanobodies. Cancer Immunol Immunother 2007;56:303-17.

21. Els Conrath K, Lauwereys M, Wyns L, Muyldermans S. Camel single-domain antibodies as modular building units in bispecific and bivalent antibody constructs. J Biol Chem 2001;276:7346-50.

22. Roovers RvD, G. A. M. S., van Bergen en Henegouwen PM. Nanobodies in therapeutic applications. Curr Opin Mol Ther 2007;9:327-35.

23. Dennis MS, Zhang M, Meng YG, Kadkhodayan M, Kirchhofer D, Combs D, Damico LA. Albumin binding as a general strategy for improving the pharmacokinetics of proteins. J Biol Chem 2002;277:35035-43.

24. Tijink BM, Laeremans T, Budde M, Stigter-van Walsum M, Dreier T, de Haard HJ, Leemans CR, van Dongen GA. Improved tumor targeting of anti-epidermal growth factor receptor Nanobodies through albumin binding: taking advantage of modular Nanobody technology. Mol Cancer Ther 2008;7:2288-97.

25. Roovers RC, Henderikx P, Helfrich W, van der Linden E, Reurs A, de Bruine AP, Arends JW, de Leij L, Hoogenboom HR. High-affinity recombinant phage antibodies to the pan-carcinoma marker epithelial glycoprotein-2 for tumour targeting. Br J Cancer 1998;78:1407-16.

26. Giard DJ, Aaronson SA, Todaro GJ, Arnstein P, Kersey JH, Dosik H, Parks WP. In vitro cultivation of human tumors: establishment of cell lines derived from a series of solid tumors. J Natl Cancer Inst 1973;51:1417-23.

27. Merlino GT, Xu YH, Ishii S, Clark AJ, Semba K, Toyoshima K, Yamamoto T, Pastan I. Amplification and enhanced expression of the epidermal growth factor receptor gene in A431 human carcinoma cells. Science 1984;224:417-9.

28. Honegger AM, Dull TJ, Felder S, Van Obberghen E, Bellot F, Szapary D, Schmidt A, Ullrich A, Schlessinger J. Point mutation at the ATP binding site of EGF receptor abolishes protein-tyrosine kinase activity and alters cellular routing. Cell 1987;51:199-209.

29. Murthy U, Basu A, Rodeck U, Herlyn M, Ross AH, Das M. Binding of an antagonistic monoclonal antibody to an intact and fragmented EGF-receptor polypeptide. Arch Biochem Biophys 1987;252:549-60.

30. Haisma HJ, Grill J, Curiel DT, Hoogeland S, van Beusechem VW, Pinedo HM, Gerritsen WR. Targeting of adenoviral vectors through a bispecific single-chain antibody. Cancer Gene Ther 2000;7:901-4.

31. De Haard HJ, Bezemer S, Ledeboer AM, Muller WH, Boender PJ, Moineau S, Coppelmans MC, Verkleij AJ, Frenken LG, Verrips CT. Llama antibodies

For Peer Review

against a lactococcal protein located at the tip of the phage tail prevent phage infection. J Bacteriol 2005;187:4531-41.

32. Hofman EG, Ruonala MO, Bader AN, van den Heuvel D, Voortman J, Roovers RC, Verkleij AJ, Gerritsen HC, van Bergen En Henegouwen PM. EGF induces coalescence of different lipid rafts. J Cell Sci 2008;121:2519-28.

33. Ferguson KM, Darling PJ, Mohan MJ, Macatee TL, Lemmon MA. Extracellular domains drive homo- but not hetero-dimerization of erbB receptors. Embo J 2000;19:4632-43.

34. Hawkins RE, Russell SJ, Winter G. Selection of phage antibodies by binding affinity. Mimicking affinity maturation. J Mol Biol 1992;226:889-96.

35. Marks JD, Hoogenboom HR, Bonnert TP, McCafferty J, Griffiths AD, Winter G. By-passing immunization. Human antibodies from V-gene libraries displayed on phage. J Mol Biol 1991;222:581-97.

36. Meulemans EV, Slobbe R, Wasterval P, Ramaekers FC, van Eys GJ. Selection of phage-displayed antibodies specific for a cytoskeletal antigen by competitive elution with a monoclonal antibody. J Mol Biol 1994;244:353-60.

37. Stemmer WP, Crameri A, Ha KD, Brennan TM, Heyneker HL. Single-step assembly of a gene and entire plasmid from large numbers of oligodeoxyribonucleotides. Gene 1995;164:49-53.

38. Sanger F, Nicklen S, Coulson AR. DNA sequencing with chain-terminating inhibitors. Proc Natl Acad Sci U S A 1977;74:5463-7.

39. Skehan P, Storeng R, Scudiero D, Monks A, McMahon J, Vistica D, Warren JT, Bokesch H, Kenney S, Boyd MR. New colorimetric cytotoxicity assay for anticancer-drug screening. J Natl Cancer Inst 1990;82:1107-12.

40. Frieden E, Lipsett MB, Winzler RJ. Methods for Labeling Thyroxine With Radioactive Iodine. Science 1948;107:353-4.

41. Visser GW, Klok RP, Gebbinck JW, ter Linden T, van Dongen GA, Molthoff CF. Optimal quality (131)I-monoclonal antibodies on high-dose labeling in a large reaction volume and temporarily coating the antibody with IODO-GEN. J Nucl Med 2001;42:509-19.

42. Coppieters K, Dreier T, Silence K, de Haard H, Lauwereys M, Casteels P, Beirnaert E, Jonckheere H, Van de Wiele C, Staelens L, Hostens J, Revets H, et al. Formatted anti-tumor necrosis factor alpha VHH proteins derived from camelids show superior potency and targeting to inflamed joints in a murine model of collagen-induced arthritis. Arthritis Rheum 2006;54:1856-66.

43. Neri D, Momo M, Prospero T, Winter G. High-affinity antigen binding by chelating recombinant antibodies (CRAbs). J Mol Biol 1995;246:367-73.

44. Cortez-Retamozo V, Lauwereys M, Hassanzadeh Gh G, Gobert M, Conrath K, Muyldermans S, De Baetselier P, Revets H. Efficient tumor targeting by single-domain antibody fragments of camels. Int J Cancer 2002;98:456-62.

45. Gainkam LO, Huang L, Caveliers V, Keyaerts M, Hernot S, Vaneycken I, Vanhove C, Revets H, De Baetselier P, Lahoutte T. Comparison of the Biodistribution and Tumor Targeting of Two 99mTc-Labeled Anti-EGFR Nanobodies in Mice, Using Pinhole SPECT/Micro-CT. J Nucl Med 2008;49:788-95.

46. Clayton A, Walker F, Orchard S, Henderson C, Fuchs D, Rothacker J, Nice E, Burgess A. Ligand-induced dimer-tetramer transition during the activation of the cell surface epidermal growth factor receptor-A multidimensional microscopy analysis. J Biol Chem 2005;280:30392-9.

47. Hofman EG, Bader AN, Voortman J, Van den Heuvel DJ, Sigismund S, Verkleij AJ, Gerritsen HC, Van Bergen En Henegouwen PM. Ligand-induced

For Peer Review

epidermal growth factor receptor (EGFR) oligomerization is kinase-dependent and enhances internalization. J Biol Chem 2010.

For Peer Review

Table 1:

Affinity characteristics and growth delay factors of different nanobodies

A. Kinetic dissociation rate constants of selected antagonistic anti-EGFR nanobodies as measured by SPR using a BIAcore

Nanobody:	k_{off} (10^{-4} s^{-1})
27H7	31.2
27E5	20.4
27C7	12.4
27E8	17.3
9G8	4.0
38G7	2.0
7C12	150
7D12	25

B Affinity values of anti-EGFR nanobodies as measured by binding of ^{125}I labelled nanobody to live cells

Nanobody:	KD (nM) on ^{14}C cells	KD (nM) on A431 cells
9G8	14.4	13.8
7D12	10.4	25.7
7D12-7D12	2.1	4.6
9G8-9G8	2.8	10.7
9G8-7D12	7.1	7.5
7D12-9G8	3.1	5.4

C Growth delay factors (GDF) for quadrupling of tumour volume after different treatments

Treatment	GDF
cetuximab	2.19
CONAN-1	1.52
7D12-7D12-Alb1	1

For Peer Review

Figure legends

Figure 1
***In vitro* characterisation of selected monovalent anti-EGFR nanobodies**
A The binding of biotinylated EGF (800pM) to an EGFR-ECD-Fc fusion was tested in the presence of increasing amounts of the 9G8, 7D12, 7C12 or 38G7 nanobodies, or without nanobody. Receptor-bound EGF was then detected via peroxydase-coupled streptavidin and staining with OPD/H_2O_2.
B-D The binding to EGFR of the 9G8, 7D12 and 9G8 nanobody respectively (B-D), expressed on phage, was detected in a 100-fold molar excess of the indicated antibody (cetuximab) or antibody fragments.

Figure 2
Inhibition of EGF-induced EGFR phosphorylation by mono- and bivalent nanobodies
EGF (8nM) was mixed with increasing amounts of nanobody (monovalent 7D12 and 9G8; bivalent 7D12 and 9G8 and bi-paratopic nanobodies 7D12-9G8 and 9G8-7D12) and the resulting mixtures were added to Her14 cells. After stimulation for 15 minutes, cell lysates were made, proteins were size-separated and blotted to PVDF membranes. Membranes were then stained for phosphorylated EGFR (Y1068) and for the total amount of tubulin as loading control.

Figure 3
Inhibition of A431 tumour cell proliferation by mono- and bivalent nanobodies
A-D The proliferation of A431 cells in the presence of increasing amounts of nanobody (A: mono- and bivalent 7D12; B: mono- and bivalent 9G8; C: mixes of mono- and bivalent 7D12 and 9G8 and D: bi-paratopic molecules 7D12-9G8 and 9G8-7D12) was measured using a sulphorhodamine-based stain of total cellular protein after TCA precipitation. Proliferation is plotted as percentage of maximal growth (cells left without treatment). The whole antibody cetuximab was used as 'standard' in every test. Data points where the value of the control is statistically different from that of the nanobody-treated group are indicated by an asterix. C: only different between 7D12+9G8 and control; D: only different between 9G8-7D12 and control.

Figure 4
***In vitro* optimalisation and characterisation of trivalent bi-paratopic nanobody CONAN-1**
A The proliferation of A431 cells in the presence of increasing amounts of bi-paratopic nanobody 7D12-9G8 (with linkers varying in length between the two nanobody units) was measured using a sulphorhodamine-based stain of total cellular protein after TCA precipitation. Proliferation is plotted as percentage of maximal growth (cells left without treatment). Error bars have been omitted to increase the clarity of the figure. The different linker lengths between the two nanobodies are indicated.
B Purified EGFR-ECD-Fc fusion protein was immobilised via a coated anti-human Fc anti-serum and a concentration range of either bivalent (7D12-9G8) or trivalent (CONAN-1) nanobody was bound. The binding of biotinylated mouse serum albumin

For Peer Review

(MSA) was subsequently detected with peroxydase-conjugated streptavidin and staining with OPD/H_2O_2.
C The proliferation of A431 cells in the presence of increasing amounts of nanobody was measured using the SRB assay. The effect of the presence of human serum albumin (HSA: 1%) in the medium was assessed.
D EGF (8nM) or nanobody (1µM) was added to serum-starved Her14 cells (-). After stimulation for 15 minutes, cell lysates were prepared, proteins were size-separated and blotted to PVDF membranes. Membranes were then stained for phosphorylated EGFR (Y1068) and for the total amount of tubulin as loading control.

E EGF (8nM) was mixed with increasing amounts of nanobody and the resulting mixture was added to Her14 cells. After stimulation for 15 minutes, cell lysates were prepared, proteins were size-separated and blotted to PVDF membranes. Membranes were then stained for phosphorylated EGFR (Y1068) and for the total amount of tubulin as loading control.

Figure 5
***In vivo* pharmacokinetics and therapy using CONAN-1 nanobody in athymic (nu/nu) mice bearing subcutaneous A431 xenografts**
A Together with a therapeutic dose of trivalent nanobody (1mg), ^{131}I-labeled CONAN-1 (7.5 µg, corresponding to 0.33 MBq) was injected intra-peritoneally (i.p.) in tumour-bearing athymic (nu/nu) mice to measure detailed blood pharmacokinetics. Blood pool radio-activity was measured in time and plotted as percentage of injected dose per gram of tissue as a function of time.

B Athymic (nude) mice bearing subcutaneously implanted A431 xenografts were treated with phosphate buffered saline (PBS; diamonds), cetuximab; barbed rounds or trivalent nanobody 7D12-9G8-Alb1 (CONAN-1; crosses). Treatment consisted of bi-weekly injections of 1mg of protein intra-peritoneally (arrows).

For Peer Review

Figure 1

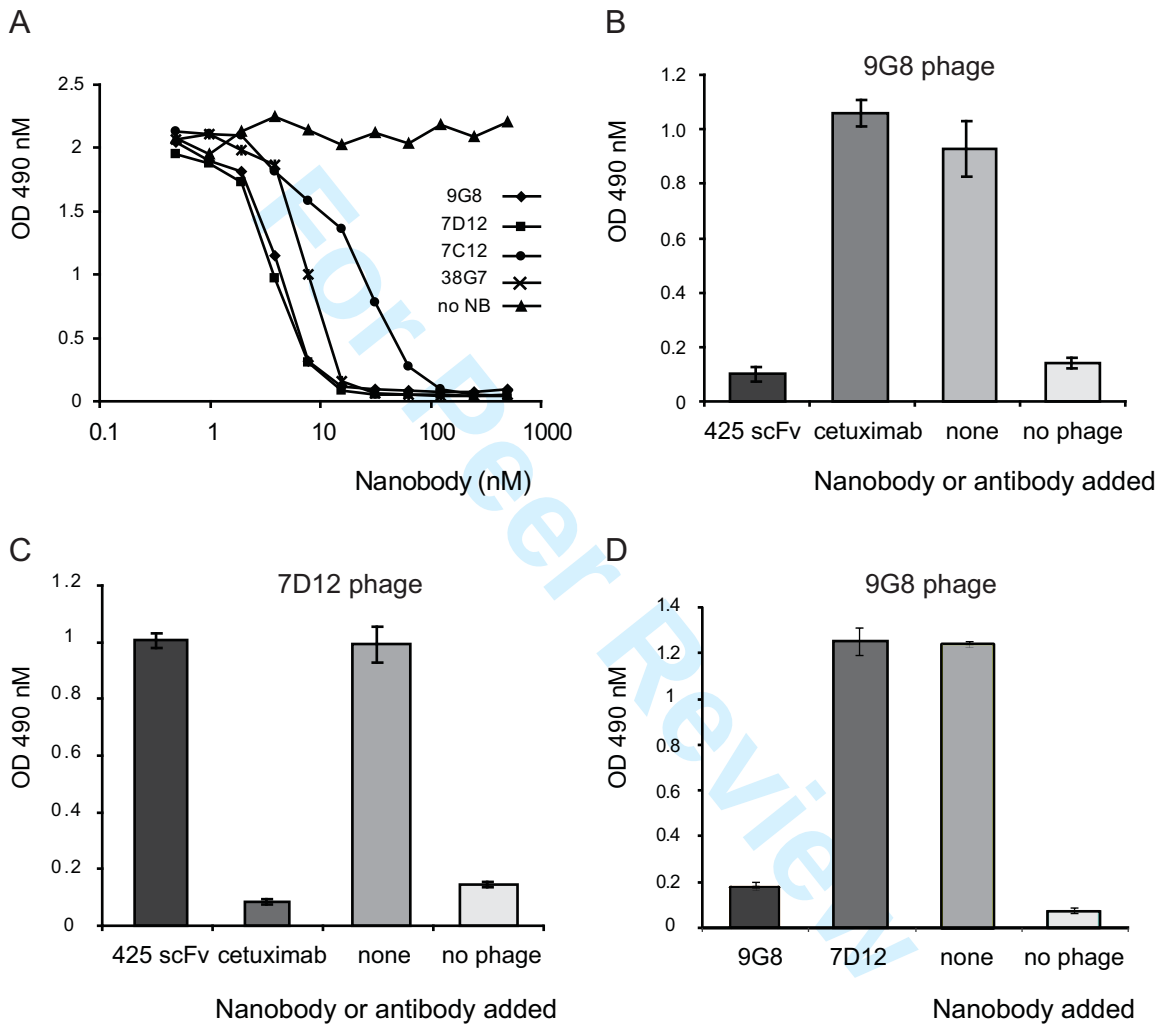

For Peer Review

Figure 2

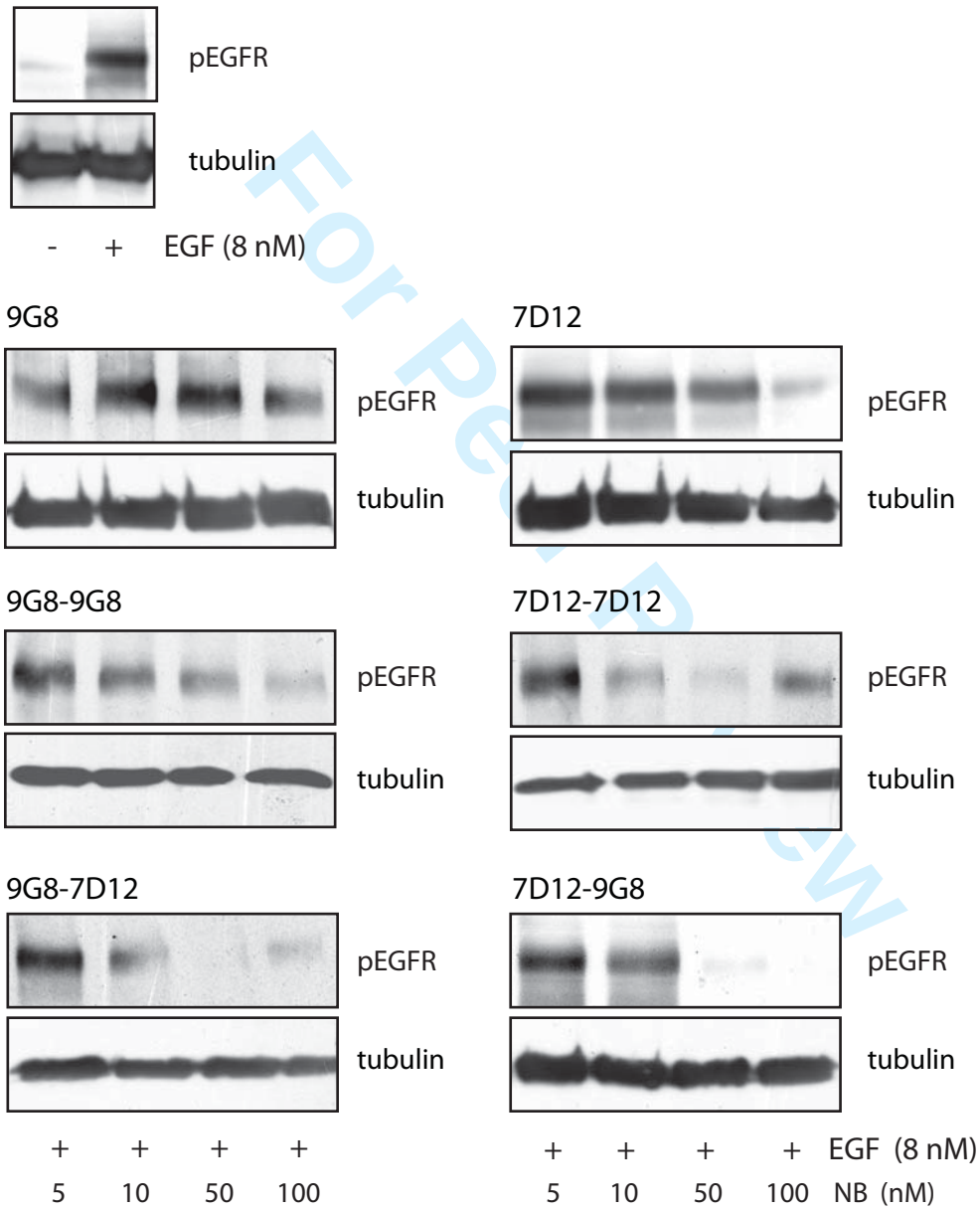

For Peer Review

Figure 3

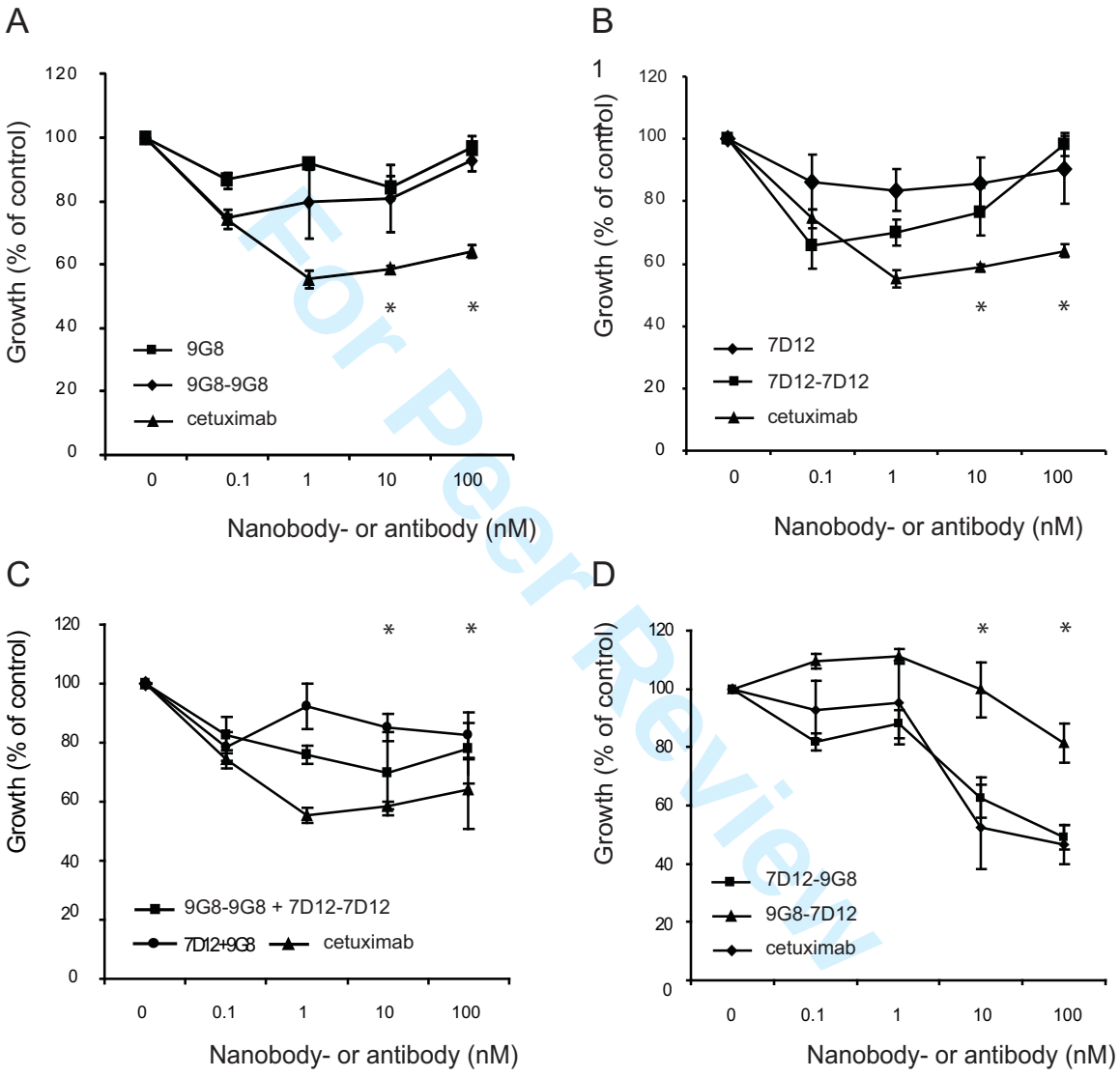

For Peer Review

Figure 4

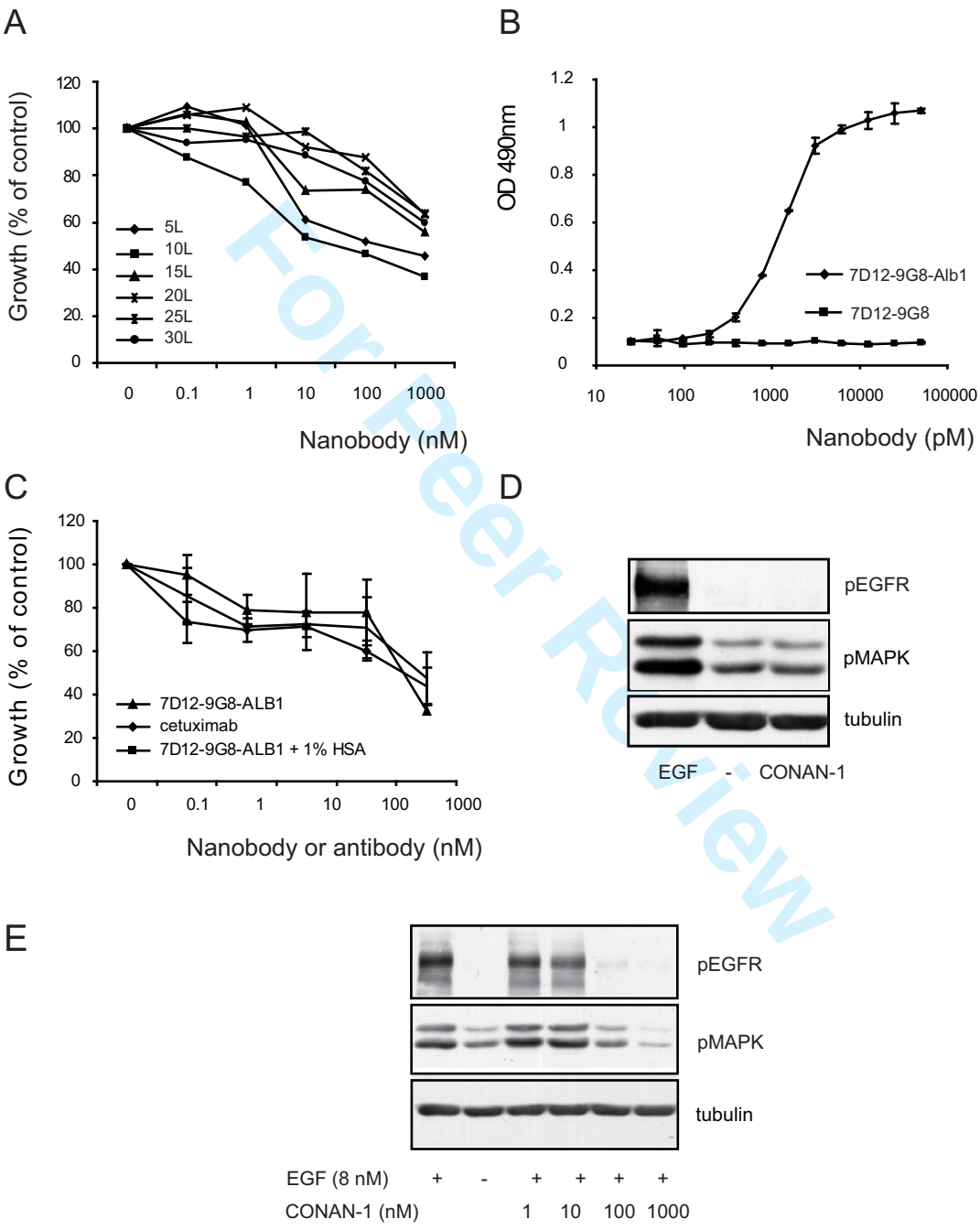

For Peer Review

Figure 5

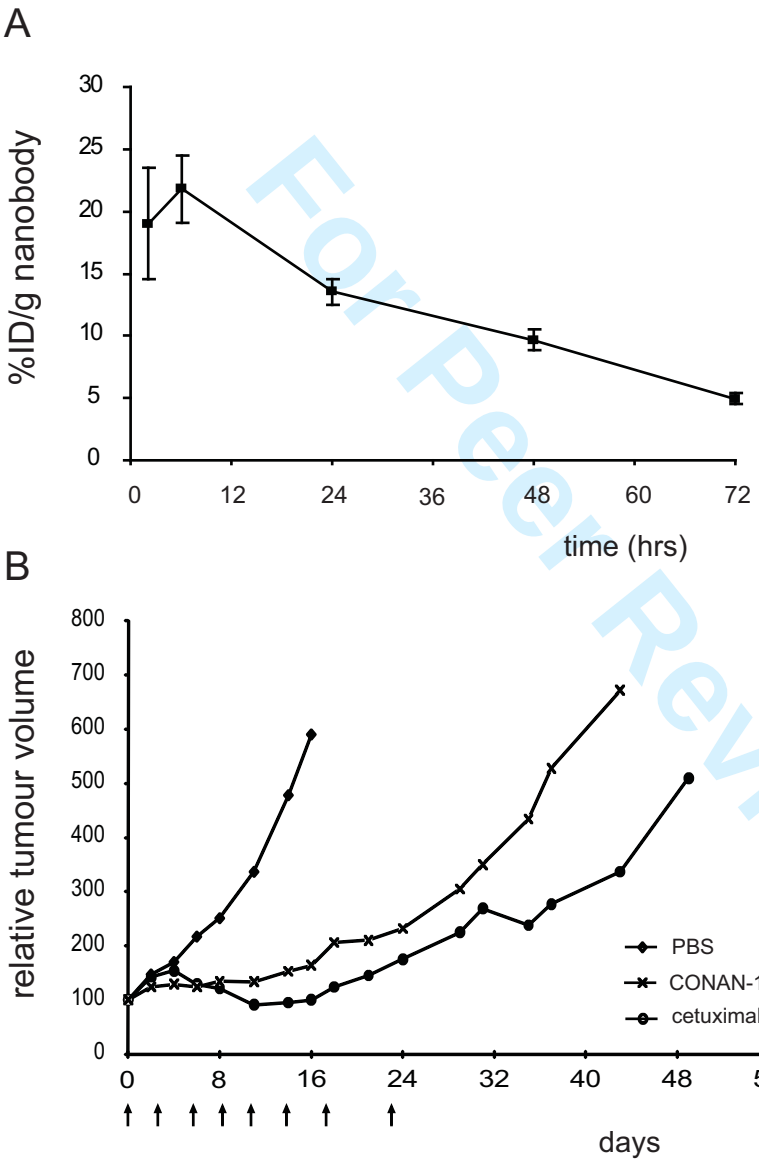

For Peer Review